

Fragmentation Atomization Mechanisms in Subsonic Cross-Flow

Xinyan Wang¹, Jiahui Zhong¹, Xinjun Zhao^{1,*}, Guang Xian²

¹ Aviation College, Inner Mongolia University of Technology, Hohhot 010051, China;

² The 41st Research Institute of the 6th Academy of China Aerospace Science and Industry Corporation, Hohhot 010010, China.

Abstract. An accurate numerical simulation of fuel atomization is realized in preparation for the study of kerosene propellant fragmentation atomization and development process under subsonic conditions in the presence of a transverse air stream. Under 11 subsonic uniform incoming air mainstream velocity conditions, a kerosene transverse jet with an average flux-to-momentum ratio $q=7.9-46$ and an average gas Weber number (Weg) ranging from 5.6 to 120 is selected to enter the air mainstream. The transverse jet under the action of the kerosene fuel under subsonic conditions is analyzed by using the Volume of Fluid Method (VFM) method the Adaptive Mesh Using the Volume of Fluid Method (VFM) and Adaptive Mesh Refinement (AMR) methods, the primary atomization phenomenon under the transverse jet is investigated, and the accuracy of the numerical simulation method is verified by comparing it with the experimental results of the previous researchers. The results show that the kerosene fuel under the action of gas film will change the time and way of droplet breakup. This process will have the participation of Rayleigh-Taylor instability and Kelvin-Helmholtz instability, and the atomization process is negatively correlated with the mean gas Weber number and positively correlated with and has a large influence on the mean flux-to-momentum ratio q .

Keywords: multiphase; primary atomization model; VOF method; kerosene propellant; Jet in a Crossflow.

1. Introduction

To reveal the fragmentation mechanism of transverse jet atomization, many scholars have carried out experimental studies on the transverse jet atomization of liquid fuel under different working conditions. The main source of liquid fragmentation is surface instability, and the surface wave mainly originates from the Rayleigh-Taylor instability, which is a hydrodynamic instability phenomenon occurring at the interface between two fluids with different densities [1], and under low Weg number conditions, the R-T instability plays a major role in the droplet fragmentation process, Joseph [2] investigated the Rayleigh-Taylor instability of viscoelastic liquids in high-velocity airflow considering fluid viscosity. The Rayleigh-Taylor stability analysis was carried out for Oldroyd B fluid and the sensitivity function of the most unstable wave was obtained. Fu [3] designed a test system for high-temperature and high-pressure jets and used the high-speed photography method to obtain the evolution law of the liquid jets under three different conditions, at the same time, the liquid jet trajectory curves were fitted, and the jet trajectory curve that can be used as a reference was obtained. R-T experiments of [4] were carried out at different liquid-to-air momentum ratio aerodynamic Weber numbers, and it was observed that the spray trajectory not only depended on the momentum ratio Q but also on the correction factor according to the value of L/D . Li [5] parametrically investigated the spraying process at different Ohnesorge and Weber numbers using the HiMIST simulation code, and the results showed that the Rayleigh-Taylor and Kelvin-Helmholtz linear stability theories are difficult to explain the different edge rupture processes and further studies are needed. In recent years, numerical simulations have been developed to some extent, and researchers [6,7] have found that the transverse flow from the nozzle to the completion of atomization mainly consists of three parts: liquid columns, liquid clumps, and liquid droplets, and the process of transforming liquid columns into liquid clumps (or large droplets) is known as the primary atomization, whereas the process of further fragmentation of the liquid

clumps (or large droplets) into even finer droplets is known as the secondary atomization. Bernard [8] investigated the primary atomization process of a turbulent liquid jet in a cross flow, the FGVT method exhibits a relatively high computational cost compared to the VOF method, but it provides a better interface resolution allowing the FGVT method to provide a more detailed interfacial profile. B [9] investigated the effect of airflow turbulence intensity on the trajectory and breakup of a liquid jet using a large eddy simulation method and found that in turbulent flow, with the transverse airflow turbulence intensity is enhanced, the energy in the fluid vortex also increases, and thus the fracture point will be close to the liquid jet location.

Previous studies may rely more on the traditional Eulerian-Lagrangian method or a single Eulerian method in simulating the propellant atomization process, which has limitations in dealing with complex two-phase flow interactions, especially the interface evolution and fragmentation details. Therefore, in this paper, the Eulerian-Eulerian model and the VOF method are applied comprehensively. Similarly, previous studies have sometimes neglected or simplified the effects of viscous effects on the flow field instabilities (e.g., K-H and R-T instabilities). This paper, on the other hand, deeply explores the influence of aviation kerosene liquid viscosity on the initial atomization morphology, reveals how viscosity affects the formation of atomization structure through accurate simulation, and provides a dynamic image of atomization that is closer to reality.

2. Physical modeling and numerical simulation conditions

2.1 Geometry Modeling and Meshing

In this paper, numerical simulation of two-dimensional transverse jet atomization under different working conditions is carried out. The computational domain is shown in Fig. 1, the two-dimensional transverse jet computational fluid region has a circular hole width of d , a pipe length of $10d$, and the main flow field is a rectangular region of $45d \times 90d$, the origin of the coordinate system is located in the center of the nozzle outlet, the kerosene propellant is ejected along the y -axis in the positive direction, and the air cross-flow is directed along the x -axis in the positive direction, and the jet channel is a circular cross-section with a width of d , and the direction of the jet velocity is at an angle of 90° to the direction of the transverse flow velocity. The direction of jet velocity is 90° from the direction of transverse flow.

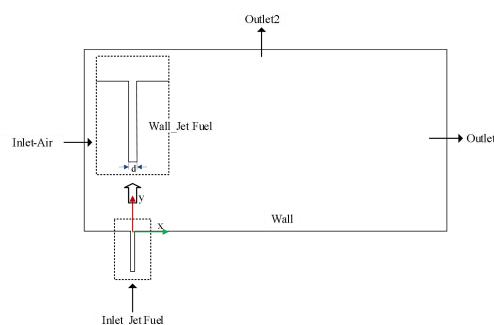


Figure. 1 Schematic diagram of the computational fluid region

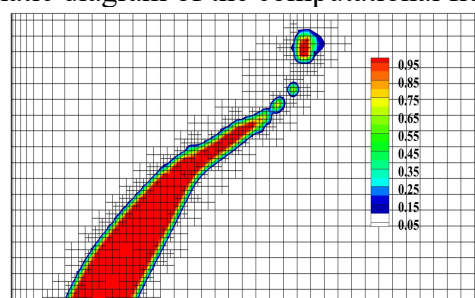


Figure. 2 Schematic diagram of the adaptive mesh during computation

ICEM was used to generate the structured mesh, and the mesh encryption of the jet inlet and boundary regions was performed by adaptive mesh encryption (AMR), as shown in Fig. 2 for the liquid-phase volume fraction of the 130,000 overall mesh in the computational process and the post-adaptive mesh, which were both performed by the second-level adaptive mesh encryption method, and the minimum mesh size after encryption was 4.29 μm .

2.2 boundary condition

In this study, the main stream is low-velocity air, the air in the transverse jet enters directly into the main stream, the air and kerosene propellant are velocity inlet, the outlet is pressure outlet, the wall is the no-slip wall, the gravitational force along the y-axis is taken into account, and the calculated working conditions are as shown in Table 1, the nozzle aperture diameter is $d=0.4\text{mm}$, the gas phase adopts the ideal air with the density of $\rho_g=1.225\text{ kg/m}^3$, and the liquid phase with the density of $\rho_l=780\text{kg/m}^3$, at $T=297.15\text{K}$, the viscosity of the gas phase is $\mu_g=1.8\times 10^{-5}\text{Pa}\cdot\text{s}$, the viscosity of the liquid phase is $\mu_l=0.0026\text{Pa}\cdot\text{s}$, the surface tension coefficient $\sigma=0.026$, and the Oh number is 0.0288.

Table 1 Calculation examples

Case	1	2	3	4	5	6	7	8	9	10	11
$U_g(\text{m/s})$	17.2	25.6	39.9	56.4	79.8	25.6	39.9	56.4	25.6	39.9	56.4
$U_l(\text{m/s})$	2.6	3.8	5.9	8.4	11.8	5.6	8.7	12.2	6.9	10.7	15.2
We_g	5.6	12.4	30	60	120	12.4	30	60	12.4	30	60
Ma	0.05	0.074	0.115	0.163	0.23	0.074	0.115	0.163	0.074	0.115	0.163
q	14	14	14	14	14	30	30	30	46	46	46

3. Findings and discussion

3.1 primary atomization process

As shown in Fig. 5, the isosurface plot of Case2 liquid phase volume fraction of 0.1 at the moment of $t=4\text{ms}$, the red curve is illustrated as the liquid jet trajectory. Combined with the pressure cloud (b) in Fig. 6, it can be observed that the liquid is accelerated by pressure through the nozzle and forms a jet, in which the kinetic energy of the liquid increases while the pressure energy decreases. From the velocity cloud (a) it can be seen that the jet forms a core region with a high flow velocity, and just after leaving the nozzle the jet, the isosurface starts to expand gradually, this is since the pressure of the surrounding gas is lower than the inside of the jet, which leads to the expansion of the jet. At the same time, the velocity in the center of the jet begins to decay, while the surrounding gas is sucked into the jet, due to the shear acceleration generated by the gas cross-flow, resulting in the generation of K-H instability along the direction of the jet, and there are constantly tiny droplets stripping. As the jet expands, its internal flow structure becomes more and more complex, R-T instability phenomenon occurs, and the jet further breaks up into smaller droplets due to surface tension, turbulence, and pressure difference when the liquid is injected into the gas medium.

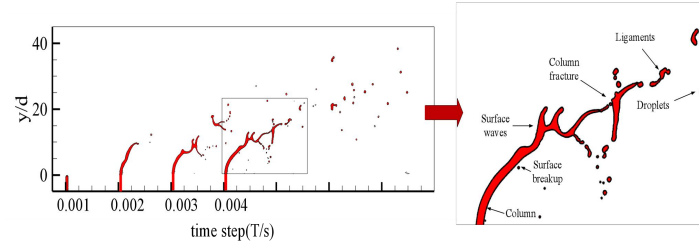


Figure. 5 Kerosene jet with time for case2 volume fraction of 0.1

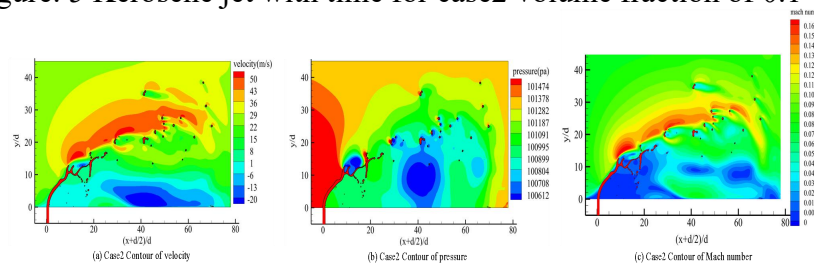


Figure. 6 Velocity, pressure and Mach number cloud diagrams

3.2 Influence of We_g on the depth of jet penetration

As can be seen from the column fragmentation point relationship Fig 7, both the column fragmentation length L_b and the penetration depth L_p decrease with the increase of We_g , where the decrease of the penetration depth L_p is accelerated between We_g of 60 and 120, because the surface wave of the liquid column changes from being dominated by the R-T instability back to being dominated by the K-H instability when the We_g increases to a certain critical value, whereas it is found that the penetration depth has a slight tendency to increase, which is different from the conclusion obtained by Chen [10], and can be attributed to the change of fragmentation mode resulting in the inability to capture the fragmentation point accurately.

The fitted curves obtained for the jet boundary at different air Weber numbers are shown in Fig. 8. The atomization boundary is generally defined as the outermost contour of the liquid mist, and the jet boundary plot is obtained by the Levenberg-Marquardt optimization algorithm, while the lower boundary contour of the liquid mist is added, which is similar to that obtained by high-fidelity numerical simulation in the related literature [5]. With the increase of the gas Weber number, the jet trajectory is shifted downward and the depth of the jet decreases, but the decrease is small. This is because when increasing the gas Weber number, the inertial force of the gas flow increases, and the differential pressure force is enhanced, at this time, the role of differential pressure force and viscous force on the jet trajectory is stronger than that of the jet inertial force, so the gas Weber number has a certain effect on the jet depth L_p , which is a key parameter in the study of transverse jet atomization.

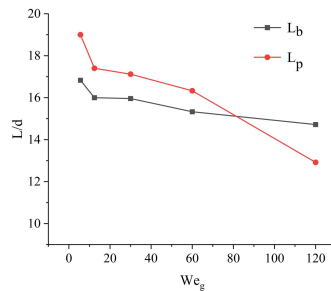


Figure. 7 Column crushing point relationship

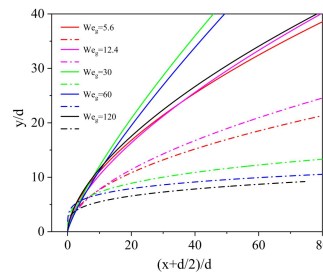


Figure. 8 Comparison of atomization boundaries

3.3 Effect of q on jet atomization patterns

As shown in Fig. 9, where the red, blue, and green colors denote the atomization trajectories at q at 14, 30, and 46 operating conditions, respectively, keeping $W_{eg} = 12.4$ and $Oh = 0.0288$ fixed, it is found that when q is small, the jet is more susceptible to the surrounding transverse airflow, leading to earlier fragmentation and smaller droplet sizes, and the droplets produced by the column fragmentation are closer to the lower wall surface, which is shown by Lin [11] concluded that the jet rapidly disperses to form a complex vortex structure and the momentum of the prevailing lateral airflow significantly exceeds that of the jet, as shown in Fig. 10.

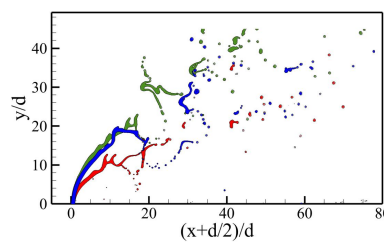


Figure. 9 Superposition of atomization patterns

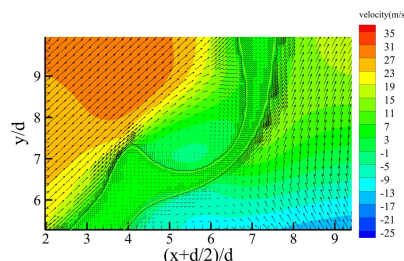


Figure. 10 case2 trough velocity vectors

Thus, the tearing and fragmentation effect of the jet by the airflow becomes more pronounced due to the vortex structure and the jet liquid is more easily captured and torn by the airflow to form finer droplets, allowing the jet to be fully atomized over a shorter distance. A high flux momentum ratio q finds that the jet maintains its integrity for a longer time and the jet has a higher momentum, which causes the jet to maintain its integrity over a longer distance, thus increasing the depth of penetration and reducing initial fragmentation.

Fig. 11 shows the plots fitted to the boundary of the kerosene liquid atomization for different flux momentum ratios, from Fig. (a), it can be seen that the penetration depth of the transverse jet is smaller at low q, where the lower boundary contour coincides with that at $q = 30$. This is because the momentum of the mainstream flow dominates the flow, which is capable of compressing or dispersing the jet more quickly and restricting the distance of its advancement, and the fragmentation of kerosene liquids is more powerful, and the formation of the droplets is smaller and more evenly distributed, the smaller droplets have a larger surface area and a faster evaporation rate, which is favorable for complete combustion. As shown in Fig. (c), as W_{eg} and q increase, the spreading range of atomization also increases, and the increase in jet penetration depth is

accompanied by higher turbulence intensity able to penetrate deeper into the mainstream gas stream.

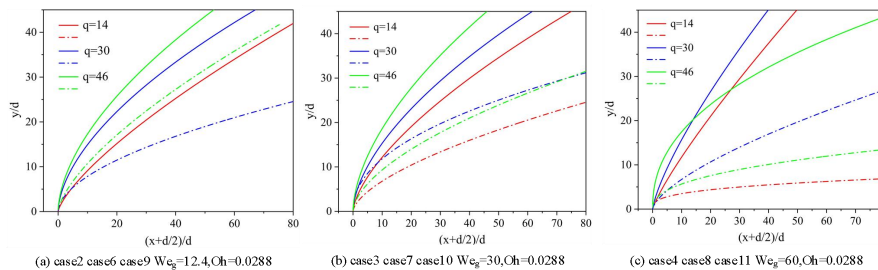


Figure 11 Comparison of liquid atomization boundaries for different flux momentum ratios

4. Conclusions

In this study, the VOF model is used to investigate the jet fragmentation mode and atomization mechanism of kerosene propellant, and the following conclusions are obtained.

(1) Broken atomization mechanism: the atomization process of kerosene propellant in subsonic transverse gas flow is mainly affected by surface tension-induced instability, especially R-T instability plays a dominant role in low gas Weber number We_g conditions, while K-H instability is more significant in high We_g conditions.

(2) The increase in the flux-to-momentum ratio helps the jet to maintain its integrity for a longer time and reduces the initial fragmentation, thus increasing the penetration depth of the jet. The tearing effect of the jet by the airflow is more significant at low q , leading to earlier fragmentation and smaller droplet sizes, which contributes to the improvement of atomization efficiency and combustion completeness.

Acknowledgements

This work is supported by the Project of Natural Science Foundation of Inner Mongolia Autonomous Region (No.2022QN01001); Project of Doctoral Foundation of Inner Mongolia University of Technology (No.BS2021013); Project of Basic Scientific Research Operating Expenses of Colleges and Universities Directly Under the Direct Subsidiary of Inner Mongolia Autonomous Region (No.JY20220183) and the Basic Research Funds for Universities directly under the Autonomous Region(Grant NO.ZTY2023025).

References

- [1] Wei Youqiang, Dong Ruoling, Zhang Yixin, et al. Study on the Interface Instability of a Shock Wave – Sub-Millimeter Liquid Droplet Interface and a Numerical Investigation of Its Breakup. *Applied Sciences*, 2023, 13(24): 13283.
- [2] JOSEPH D D, BEAVERS G S, FUNADA T. Rayleigh – Taylor instability of viscoelastic drops at high Weber numbers. *Journal of Fluid Mechanics*, 2002, 453: 109-132.
- [3] Fu Benshuai, Lu Bingju, Xiao Haiyan, et al. Experimental research on the atomization of transverse liquid jet. *Journal of Physics: Conference Series*, 2024, 2764(1): 012049.
- [4] SURYA PRAKASH R, SINHA A, TOMAR G, et al. Liquid jet in crossflow – Effect of liquid entry conditions. *Experimental Thermal and Fluid Science*, 2018, 93: 45-56.
- [5] Li Xiaoyi, Gao Hui, MARIOS C. SOTERIOU. Investigation of the impact of high liquid viscosity on jet atomization in crossflow via high-fidelity simulations. *Physics of Fluids*, 2017, 29(8): 082103.
- [6] LIU A, MATHER D, REITZ R. Modeling the Effects of Drop Drag and Breakup on Fuel Sprays. *SAE Technical Papers*, 1993: 17.

- [7] IM K S, LIN K C, LAI M C, et al. Breakup modeling of a liquid jet in cross flow. *International Journal of Automotive Technology*, 2011, 12(4): 489-496.
- [8] BERNARDO ALAN DE FREITAS DUARTE, FRANCO BARBI, MILLENA MARTINS VILLAR, et al. Primary atomization of a turbulent liquid jet in crossflow: a comparison between VOF and FGVT methods. *Journal of the Brazilian Society of Mechanical Sciences and Engineering*, 2020, 42(6): 277.
- [9] JALILI B, JALILI P. Numerical analysis of airflow turbulence intensity effect on liquid jet trajectory and breakup in two-phase cross flow. *Alexandria Engineering Journal*, 2023, 68: 577-585.
- [10] Chang Jianlong, Chen Lianhua, Zhao Yongjuan et al. Analysis on research status of droplet atomization of jet in crossflow. *Tactical Missile Technology*, 2022,(2): 29-36+82.
- [11] Lin Sen, Shen Chibing, Xiao Feng, et al. Large Eddy Simulation of Primary Breakup of Transverse Pulsed Liquid Jet in Supersonic Flow. *Journal of Combustion Science and Technology*, 2020, 26(1): 87-95